Inorg. Chem. **2009**, *48*, 4075−4082

Photochemical Study on the Reactivity of Tetrasulfur Tetranitride, S_4N_4

Elena A. Pritchina,[†,‡] Nina P. Gritsan,[*,†,§] Andrey V. Zibarev,[§,∥] and Thomas Bally[*,⊥]

Institute of Chemical Kinetics & Combustion and Institute of Organic Chemistry, Siberian Branch of the Russian Academy of Sciences, Novosibirsk, Russia, Department of Natural Sciences and Department of Physics, Novosibirsk State University, Novosibirsk, Russia, and Department of Chemistry, University of Fribourg, Switzerland

Received November 10, 2008

To elucidate the multifaceted but poorly understood chemistry of the pivotal polysulfur−nitrogen heterocycle, tetrasulfur tetranitride (S_4N_4, **1**), its photochemistry was studied in Ar matrices. Thereby two primary intermediates and a secondary one (**2**−**4**) were detected, and their UV−vis and IR spectra were identified through specific interconversions of **1**−**4** that can be induced by selective irradiations. The structures associated with these spectra were assigned with the help of DFT calculations. From these assignments it follows that, under the conditions of the present experiments, the cage structure of **1** transforms into isomeric structures **2**−**4**, one of which is a boat-shaped 8-membered cycle (**2**), and the two other are novel 6-membered S_3N_3 cycles carrying exocyclic (N)—S≡N (**3**) or (S)—N═S (**4**) groups, respectively, which have not been previously described. These three intermediates probably play a pivotal role in the formation of the diverse products that are observed in the reactions of S_4N_4 even under mild reaction conditions.

Introduction

Tetrasulfur tetranitride, S_4N_4 (**1**, Chart 1), is one of the most interesting species in the context of structure, bonding, and reactivity of main-group inorganic compounds.[1] Discovered in 1835, that is, only 10 years after the discovery of benzene,[2] the compound has since been the subject of extensive studies.[1] Its rather peculiar, highly symmetric cage structure (D_{2d}),[3] as well as several aspects of its electronic structure[3c,4] have been and still are a matter of debate.

Chart 1

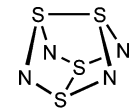

1

Over time, the above studies[1] revealed a very high and varied chemical reactivity of **1** which is nowadays described, in part, in practically every contemporary textbook on main-group inorganic chemistry. These findings comprise a significant part of the extremely broad, fascinating, and practically important field of modern chalcogen−nitrogen

* To whom correspondence should be addressed. E-mail: gritsan@kinetics.nsc.ru (N.P.G.); thomas.bally@unifr.ch (T.B.).
† Institute of Chemical Kinetics and Combustion, Russian Academy of Sciences.
‡ Department of Natural Sciences, Novosibirsk State University.
§ Department of Physics, Novosibirsk State University.
∥ Institute of Organic Chemistry, Russian Academy of Sciences.
⊥ University of Fribourg.

(1) (a) Becke-Goehring, M. *Prog. Inorg. Chem.* **1959**, *1*, 207–235. (b) Becke-Goehring, M.; Jolly, W. L.; Camp, U. C.; Macomber, J. D.; Woeller, H. F. *Inorg. Syn.* **1960**, *6*, 123–128. (c) Heal, H. G. *Adv. Inorg. Chem. Radiochem.* **1972**, *15*, 375–412. (d) Heal, H. G. *The Inorganic Heterocyclic Chemistry of Sulfur, Nitrogen and Phosphorus*; Academic Press: London, 1980. (e) Chivers, T. *Chem. Rev.* **1985**, *85*, 341–365. (f) Cotton, F. A.; Wilkinson, G. *Advanced Inorganic Chemistry*; Wiley: New York, 1988. (g) Chivers, T.; Hilts, R. W. *Coord. Chem. Rev.* **1994**, *137*, 201–232. (h) Wiberg, N. *Holleman-Wiberg Lehrbuch der Anorganischen Chemie*; Walter de Gruyter: Berlin, 1995; (i) Greenwood, N. N.; Earnshaw, A. *Chemistry of the elements*; Butterworth-Heinemann: Oxford, 1997. (j) Chivers, T. *A Guide to Chalcogen-Nitrogen Chemistry*; World Scientific: London, 2005.
(2) (a) Gregory, W. *J. Pharm.* **1835**, *21*, 315. (b) Gregory, W. *J. Pharm.* **1835**, *22*, 301.
(3) (a) Clark, D. *J. Chem. Soc.* **1952**, 1615–1620. (b) Sharma, B. D.; Donohue, J. *Acta Crystallogr.* **1963**, *16*, 891–897. (c) DeLucia, M. L.; Coppens, P. *Inorg. Chem.* **1978**, *17*, 2336–2338. (d) Almond, M. J.; Forsyth, G. A.; Rice, D. A.; Downs, A. J.; Jeffery, T. L.; Hagen, K. *Polyhedron* **1989**, *8*, 2631–2636. (e) Irsen, S. H.; Jacob, P.; Dronskowski, R. *Z. Anorg. Allg. Chem.* **2001**, *627*, 321–325. (f) Chung, G.; Lee, D. *J. Mol. Struct.: Theochem* **2002**, *582*, 85–90.
(4) (a) Gleiter, R. *J. Chem. Soc. (A)* **1970**, 3174–3179. (b) Salaneck, W. R.; Lin, J. W.; Paton, A.; Duke, C. B.; Ceasar, G. P. *Phys. Rev. B.* **1976**, *13*, 4517–4528. (c) Gleiter, R. *Angew. Chem.* **1981**, *20*, 444–452. (d) Suontamo, R. J.; Laitinen, R. S. *J. Mol. Struct.: Theochem* **1995**, *336*, 55–60. (e) Scherer, W.; Spiegler, M.; Pedersen, B.; Tafipolsky, M.; Hieringer, W.; Reinhard, B.; Downs, A. J.; McGrady, G. S. *Chem. Commun.* **2000**, 635–636.

10.1021/ic802145x CCC: $40.75
Published on Web 04/01/2009

chemistry[1j] for which **1** is one of the cornerstone compounds. It is known that electrochemical reduction of **1** yields six-membered ring $[S_3N_3]^-$compounds.[1j,5] Ring contraction is also a common reaction of S_4N_4 under the impact of nucleophilic or reducing reagents.[1j,6] Reduction leads to the population of the π^* LUMO, which promotes ring cleavage followed by recyclization to six-membered rings. By analogy, photochemical activation of **1** is also expected to promote ring opening and subsequent recyclization.

Despite the fact that **1** is widely used in numerous inorganic and organoelement syntheses, the rich reactivity of **1** is far from being well-understood. Thus, elucidating the chemical reactivity of **1** is a timely scientific challenge. One way to approach this problem is to investigate first the chemical behavior of **1** in the absence of other reagents, that is, if it is exposed to thermal or light energy under well-controlled conditions which allow the characterization of the primary or secondary intermediates that presumably engage in subsequent bimolecular reactions of S_4N_4.

Thermal transformations of **1** have already received some attention, especially in connection with its silver-wool catalyzed gas-phase cracking to give S_2N_2 which spontaneous polymerization provides $(SN)_x$.[1] The photoinduced low-temperature solution polymerization of S_2N_2 is an alternative source of $(SN)_x$[7] which is among the best known molecular (polymeric) conductors and low-temperature ($T_c = 0.3$ K) superconductors.[7,8] Pyrolysis of **1** in an inert atmosphere leads to its decomposition into the elements,[9] whereas in CS_2 solution, and in the presence of sulfur, thermolysis of **1** at 100−120 °C gives mostly S_4N_2 and N_2.[1a−c] However, it is difficult to conduct mechanistic studies under the conditions used in the above thermal transformations. In this context, photochemistry provides better opportunities.

Although rather rarely used for synthetic purposes, photochemical methods have proven to be very helpful for elucidating reaction mechanisms. The techniques of laser flash and low-temperature photolysis in combination with that of matrix isolation very frequently provide direct information on the identity, the properties, and the reactivities of reaction intermediates. In cases where thermal and photochemical reactions result in similar products, it is assumed that the reaction intermediates are very likely the same. In this way one can learn much in the way of understanding chemical reactivity.

The gas-phase photodissociation of **1** was studied using KrF (248 nm) and KrCl (222 nm) excimer lasers.[10] For excitation at 248 nm, it was hypothesized that a two-photon absorption promotes the ground singlet state of **1** to an upper repulsive singlet state which rapidly dissociates to an acyclic S_3N_3 and a vibrationally excited $[NS]^\bullet$ radical.[10]

There is only one report devoted to the solution photochemistry of **1**.[11] Its authors demonstrated that photolysis of a mixture of **1** and $[PtCl_2(PMe_2Ph)_2]$, similar to its thermolysis, resulted in the formation of the metal−sulfur−nitrogen complexes $[Pt(S_2N_2H)Cl(PMe_2Ph)_2]$ and $[Pt(S_3N)Cl(PMe_2Ph)_2]$ along with a number of unidentified phosphine−sulfur−nitrogen species. On the other hand, the products of the photolysis of **1** in the absence of metal species depended both on the concentration of S_4N_4 and on the solvent: preparative photolysis of a saturated solution of **1** in cyclohexane gave mainly colored S_4N_2 as well as S_8 and S_7NH, whereas photolysis in CH_2Cl_2 and MeOH resulted in complete decoloration with formation of S_7NH in the latter solvent. In addition, the solution photolysis of a 1:2 adduct of **1** with norbornadiene has been also studied and shown to give persistent radicals detected by EPR.[12]

Application of photochemical methods to elucidate the chemistry of other chalcogen−nitrogen compounds, such as the broad family of C, N, and S compounds, is also quite rare, both in the context of preparative[13] and mechanistic[14] investigations. Nevertheless, these studies revealed a common trend of sulfur−nitrogen π-heterocycles to form stable thiazyl π-radicals on photolysis.[14] For instance, photolysis of 1,3,2,4-benzodithiadiazines and 1,2,4,3,5-benzotrithiadiazepines in dilute hydrocarbon solutions leads to 1,2,3-benzodithiazolyls (Herz radicals), whereas that of Ar-CN_5S_3 bicycles leads to 4-Ar-1,2,3,5-dithiadiazolyls (Chart 2), in all cases in nearly quantitative yields.[14] With the help of matrix isolation spectroscopy, the primary photochemical process for 1,3,2,4-benzodithiadiazine was recently identified as the cleavage of a weak SN bond which is followed by secondary reactions that lead to a number of intermediates that were also detected.[14e]

The present work is devoted to the study of the photochemistry of **1** in argon matrices. The products of the primary

(5) Chivers, T.; Hojo, M. *Inorg. Chem.* **1984**, *23*, 1526–1530.
(6) (a) Bojes, J.; Chivers, T. *J. Chem. Soc., Chem. Commun.* **1977**, 453–454. (b) Bojes, J.; Chivers, T.; Drummond, I.; MacLean, G. *Inorg. Chem.* **1978**, *17*, 3668–3672. (c) Chivers, T.; Oakley, R. T. *Top. Curr. Chem.* **1982**, *102*, 119–147.
(7) Labes, M. M.; Love, P.; Nichols, L. F. *Chem. Rev.* **1979**, *79*, 1–15.
(8) (a) Walatka, V. V.; Labes, M. M.; Perlstein, J. H. *Phys. Rev. Lett.* **1973**, *31*, 1139–1142. (b) Green, R. L.; Street, G. B.; Suter, L. J. *Phys. Rev. Lett.* **1975**, *34*, 577–579. (c) Banister, A. J.; Correl, I. B. *Adv. Mater.* **1998**, *10*, 1415–1429. (d) Kurmaev, E. Z.; Poteryaev, A. I.; Anisimov, V. I.; Karla, I.; Moewes, A.; Schneider, B.; Neumann, M.; Ederer, D. L.; Lyubovskaya, R. N. *Physica C* **1999**, *321*, 191–198.
(9) (a) Barker, C. K.; Cordes, A. W.; Margrave, J. L. *J. Phys. Chem.* **1965**, *69*, 334–335. (b) Kudo, Y.; Hamada, S. *Bull. Chem. Soc. Jpn.* **1983**, *56*, 2627–2630. (c) Bock, H.; Solouki, B.; Roesky, H. W. *Inorg. Chem.* **1985**, *24*, 4425–4427.
(10) (a) Henshaw, T. L.; Ongstad, A. P.; Lawconell, R. I. *J. Chem. Phys.* **1992**, *96*, 53–66. (b) Ongstad, A. P.; Lawconell, R. I.; Henshaw, T. L. *J. Chem. Phys.* **1992**, *97*, 1053–1064.
(11) Allen, C. W.; Kelly, P. F.; Woollins, J. D. *J. Chem. Soc., Dalton Trans.* **1991**, *134*, 1343–1345.
(12) (a) Brinkman, M. R.; Sutcliffe, L. H. *J. Magn. Reson.* **1977**, *28*, 263–270. (b) Rolfe, S.; Griller, D.; Ingold, K. U.; Sutcliffe, L. H. *J. Org. Chem.* **1979**, *44*, 3515–3519.
(13) (a) Morris, J. L.; Rees, C. W. *J. Chem. Soc., Perkin Trans. 1* **1987**, 217–223. (b) Pavlik, J. W.; Changtong, C.; Tsefrikas, V. M. *J. Org. Chem.* **2003**, *68*, 4855–4861.
(14) (a) Vlasyuk, I. V.; Bagryansky, V. A.; Gritsan, N. P.; Molin, Yu. N.; Makarov, A. Yu.; Gatilov, Yu. V.; Scherbukhin, V. V.; Zibarev, A. V. *Phys. Chem. Chem. Phys.* **2001**, *3*, 409–415. (b) Shuvaev, K. V.; Bagryansky, V. A.; Gritsan, N. P.; Makarov, A. Yu.; Molin, Yu. N.; Zibarev, A. V. *Mendeleev Commun.* **2003**, *13*, 178–179. (c) Gritsan, N. P.; Kim, S. N.; Makarov, A. Yu.; Chesnokov, E. N.; Zibarev, A. V. *Photochem. Photobiol. Sci.* **2006**, *5*, 95–101. (d) Gritsan, N. P.; Shuvaev, K. V.; Kim, S. N.; Knapp, C.; Mews, R.; Bagryansky, V. A.; Zibarev, A. V. *Mendeleev Commun.* **2007**, *17*, 204–206. (e) Gritsan, N. P.; Pritchina, E. A.; Bally, T.; Makarov, A. Yu.; Zibarev, A. V. *J. Phys. Chem. A* **2007**, *111*, 817–824.

Chart 2

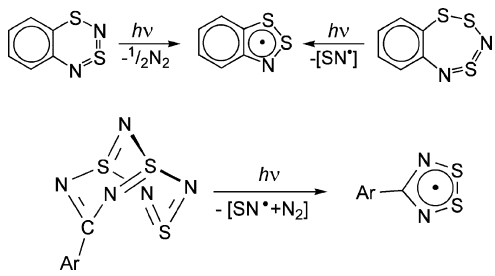

photochemical bond cleavage, as well as the products of further transformations, were detected. The molecular structures of these intermediates were assigned on the basis of their IR and UV−vis spectra and corresponding quantum chemical calculations.

Experimental and Computational Details

Compound **1** was synthesized and purified following the published procedures, mp 185−186 °C (decomposition; ***Caution! the compound is explosive***).[15] The photolysis of hexane solutions of **1** was performed using the 254 nm line of a low-pressure Hg lamp equipped with a combination of UV and gaseous Cl_2 filters. The quantum yield of photolysis was measured using the isomerization of 2-morpholino-1,4-naphthoquinone as an actinometric photoreaction with a quantum yield of 0.24 at 254 nm in hexane.[16]

Spectroscopy in Argon Matrices.[17] A few crystals of 1 were cautiously ground and placed in a U-tube attached to the inlet system of the cryostat. A mixture of argon with 10% nitrogen (which is added to improve the optical quality of matrices) was flowed through the U-tube and slowly deposited on a CsI window (UV transparent quality, Korth Kristalle GmbH) maintained at approximately 20 K. During deposition the temperature of the U-tube was kept at about 40 °C. After deposition the matrix was cooled to the lowest limit attainable by the closed-cycle cryostat (ca. 12 K).

Photolysis of **1** was performed with a low-pressure mercury lamp (254 nm) or a medium-pressure Hg/Xe lamp with a 365 nm interference filter. Subsequent irradiations were effected using the medium-pressure Hg/Xe lamp and appropriate interference and cutoff filters as described in the Results section. Electronic absorption spectra were obtained on a Perkin-Elmer Lambda 900 spectrometer (200−1000 nm). IR spectra were measured on a Bomem DA3 interferometer (4000−500 cm^{-1}) with an MCT detector.

Quantum Chemical Calculations. The geometries and harmonic vibrational frequencies of **1** and the presumed intermediates of its photolysis were calculated by the B3LYP[18] density functional method using Dunning's correlation-consistent triple-ζ basis set (cc-pVTZ). All equilibrium structures were ascertained to be minima on the potential energy surfaces. The harmonic frequencies calculated at the B3LYP/cc-pVTZ level were used without scaling in assigning the experimental IR spectra.

Excited state energies of **1** and proposed intermediates were calculated at the B3LYP/cc-pVTZ geometries by the time-dependent TD-B3LYP/aug-cc-pVTZ method.[19] All calculations were performed with the Gaussian 03[20] suite of programs. The influence of the argon on the electronic absorption spectra was taken into account by the PCM[21] model as implemented to Gaussian 03.

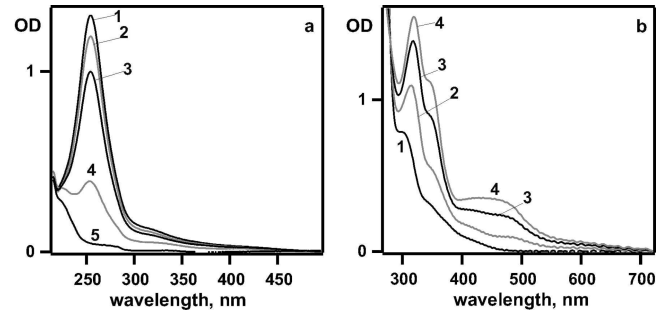

Figure 1. (a) UV−vis spectra obtained after photolysis of **1** at 254 nm for 0 min (1), 5 min (2), 13 min (3), 45 min (4), and 128 min (5) in 7.2×10^{-5} M hexane solution saturated by argon at 298 K. (b) UV−vis spectra obtained after photolysis of **1** at 254 nm for 0 min (1), 1.5 min (2), 6 min (3), and 15 min (4) in an argon matrix at 12 K.

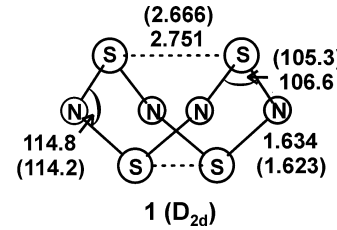

Figure 2. D_{2d} structure of **1** optimized at the B3LYP/cc-pVTZ level of theory. The experimental gas phase bond lengths (in Å) and angles (in degrees) are given in parentheses.[3d]

Results and Discussion

Figure 1a demonstrates that room-temperature irradiation of a degassed hexane solution of **1** at 254 nm leads to its decomposition with a very low quantum yield (0.009 ± 0.002). The products of this decomposition have no noticeable absorption above 250 nm (Figure 1a), whereas tetrasulfur dinitride, S_4N_2, which was formed upon photolysis of saturated solution of **1** in cyclohexane,[11] has intense bands in near-UV and visible regions ($\lambda_{max}(\log \varepsilon) = 377$ (3.38) and 455 nm (3.08)).[22] Note that similar decoloration was observed earlier upon irradiation of dilute solutions of **1** in CH_2Cl_2 and MeOH.[11] In our opinion, the formation of S_4N_2 in saturated solutions[11] was caused by a high concentration of **1** and very long time of preparative photolysis (24 h). Note that we were also unable to detect any EPR signals upon photolysis of hexane solutions of **1**.

(15) (a) Villena-Blanco, M.; Jolly, W. L. *Inorg. Synth.* **1967**, *9*, 98–102. (b) Makarov, A. Yu.; Bagryanskaya, I. Yu.; Gatilov, Yu. V.; Mikhalina, T. M.; Shakirov, M. M.; Shchegoleva, L. N.; Zibarev, A. V. *Heteroatom Chem.* **2001**, *12*, 563–576. (c) Maaninen, A.; Siivari, J.; Laitinen, R. S.; Chivers, T. *Inorg. Synth.* **2002**, *33*, 196–199.
(16) (a) Gritsan, N. P.; Bazhin, N. M. *Bull. Acad. Sci. USSR, Div. Chem. Sci.* **1980**, *29*, 897–902. (b) Gritsan, N. P.; Bazhin, N. M. *Bull. Acad. Sci. USSR, Div. Chem. Sci.* **1981**, *30*, 210–214.
(17) Bally, T. In *Reactive Intermediate Chemistry*; Moss, R. A., Platz, M. S., Jones, M., Eds.; Wiley-Interscience: New York, 2004; pp 797845.
(18) (a) Becke, A. D. *J. Chem. Phys.* **1993**, *98*, 5648–5652. (b) Lee, C.; Yang, W.; Parr, R. G. *Phys. Rev. B* **1988**, *37*, 785–789.
(19) Dreuw, A.; Head-Gordon, M. *Chem. Rev.* **2005**, *105*, 4009–4037.
(20) Frisch, M. J. A.; et al. *Gaussian 03*, Revision B.01); Gaussian, Inc.: Pittsburg, 2003 (Full reference is given in Supporting Information).
(21) Tomasi, J.; Mennucci, B.; Cammi, R. *Chem. Rev.* **2005**, *105*, 2999–3093.
(22) (a) Nelson, J.; Heal, H. G. *J. Chem. Soc. A* **1971**, 136–139. (b) Chivers, T.; Codding, P. W.; Laidlaw, W. G.; Liblong, S. W.; Oakley, R. T.; Trsic, M. *J. Am. Chem. Soc.* **1983**, *105*, 1186–1192.

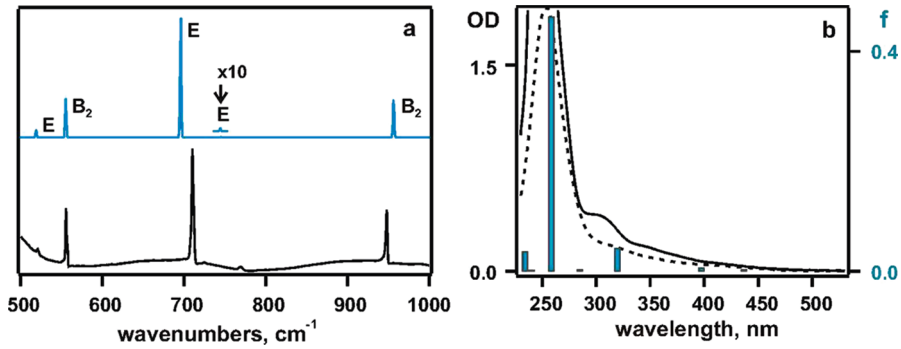

Figure 3. (a) Experimental IR spectrum of **1** in an argon matrix at 12 K (black) and its simulation by the B3LYP/cc-pVTZ method (blue). (b) UV−vis spectrum of **1** in an argon matrix at 12 K (solid) and in hexane solution at 298 K (dashed). The vertical blue bars indicate the positions and oscillator strengths of electronic transitions calculated by the TD-B3LYP/aug-cc-pVTZ method at the B3LYP/cc-pVTZ geometry of **1**.

Table 1. Vertical Excitation Energies (E) and Oscillator Strengths (f) of **1** Calculated by the B3LYP/aug-cc-pVTZ//B3LYP/cc-pVTZ Method in Argon

electronic transition	E, eV	λ, nm	f	major configurations
$1^1A_1 \rightarrow 1^1E$	2.83	437	0.0022	46% $8b_2 \rightarrow 12e$ + 45% $3a_2 \rightarrow 12e$
$1^1A_1 \rightarrow 2^1E$	3.12	398	0.0056	30% $8b_2 \rightarrow 12e$ − 41% $3a_2 \rightarrow 12e$ + 24% $9a_1 \rightarrow 12e$
$1^1A_1 \rightarrow 3^1E$	3.87	320	0.0416	38% $9a_1 \rightarrow 12e$ + 41% $4b_1 \rightarrow 12e$
$1^1A_1 \rightarrow 4^1E$	4.34	286	0.0022	23% $4b_1 \rightarrow 12e$ + 68% $7b_2 \rightarrow 12e$
$1^1A_1 \rightarrow 5^1E$	4.79	259	0.4616	21% $9a_1 \rightarrow 12e$ − 23% $4b_1 \rightarrow 12e$ + 18% $7b_2 \rightarrow 12e$

In contrast, new products showing absorptions in the near-UV and visible regions were observed upon 254 nm irradiation of **1** embedded in an argon matrix at 12 K (Figure 1b).

As we intended to assign the IR and UV−vis spectra detected upon photolysis of **1** in argon matrices by means of quantum chemical calculations, we began by testing the accuracy and reliability of the methods we wanted to use by reproducing the IR and UV−vis spectra of **1**. The structure of **1** was optimized at the B3LYP/cc-pVTZ level (Figure 2) which resulted in a cage structure of D_{2d} symmetry with the bond lengths and bond angles close to those determined experimentally in crystalline state[3c] and in the gas phase,[3d] although the calculated S−S bond lengths are noticeably longer than the experimental ones. Note that the geometries of **1** optimized earlier by the MP2, MP4, and B3LYP methods with 6-31+G(d) basis are in poorer agreement with experiment.[3f]

The IR spectrum of **1** calculated at the same level is also found to be in very good agreement with experiment (Figure 3a). Note that the previous assignment[23] of the IR band at 938 cm^{-1} to a stretching mode of E symmetry and that at 705 cm^{-1} to the B_2 stretching mode had apparently been incorrect. Figure 3b and Table 1 show that TD-DFT calculations reproduce the UV−vis spectrum of **1** very well. Therefore, it appears that this computational protocol can be used with confidence for spectral assignments of products formed upon photolysis of **1**.

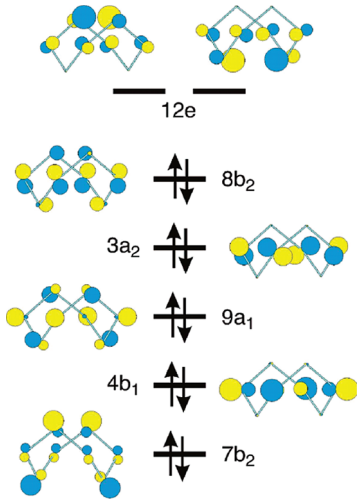

Figure 4. Molecular orbitals of **1** involved in the first five electronic transitions (Table 1).

Table 1 shows that the first five electronic transitions of **1** consist mainly of electron promotions from the five highest occupied orbitals ($8b_2$, $3a_2$, $9a_1$, $4b_1$, and $7b_2$, Figure 4) to the same doubly degenerate LUMO (12e). This LUMO may be characterized as a combination of the σ^*(S−S) and the allylic π^*(S−N) orbitals (Figure 4). In contrast, the HOMO ($8b_2$) has a σ(S−S) bonding contribution while the other orbitals involved in the observed transitions are mixtures of essentially nonbonding orbitals localized on S and N atoms. The weak nature of the S−S σ-bonds (i.e., small gap between σ-bonding and σ^*-antibonding levels) in **1** are the reason for the low energy of the first two transitions.

Figures 5a,b show the complicated pattern of spectral changes in the UV−vis and IR ranges, respectively, which is observed on photolysis of **1** in an argon matrix. Brief irradiation at 254 nm resulted in the formation of an intermediate with an absorption maximum at ca. 320 nm (Figure 5a, spectrum 1). Simultaneously, the strong IR bands of **1** diminished and gave way to a set of new, weaker peaks (Figure 5b, trace 1). Further irradiation at 254 nm (Figure 5a, spectra 2−6) led to the growth of absorptions with maxima at 345 and ca. 450 nm, along with a band peaking at ca. 320 nm. Figure 5b shows that these irradiations also gave rise to a set of IR peaks (spectra 3 and 5) similar to those detected after the brief first irradiation but differing in their relative intensities.

(23) (a) Bragin, J.; Evans, M. V. *J. Chem. Phys.* **1969**, *51*, 268–277. (b) Turowski, A.; Appel, R.; Sawodny, W.; Molt, K. *J. Mol. Struct.* **1978**, *48*, 313–323.

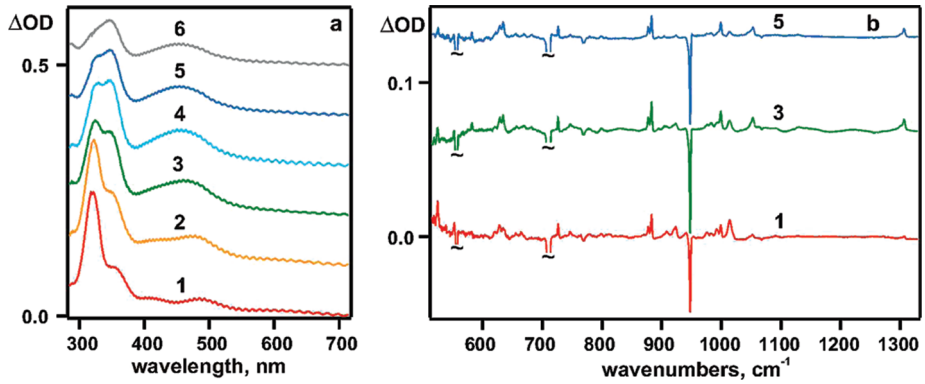

Figure 5. (a) The sequence of difference UV−vis (a) and IR (b) spectra obtained after photolysis of **1** at 254 nm for 40 s (1) and next 50 s (2), 1.5 min (3), 3 min (4), 4 min (5), and 5 min (6) in an argon matrix at 12 K. The most intense IR bands of **1** at 555 and 710 cm^{-1} are truncated. Similar UV−vis and IR spectra were observed upon irradiation of **1** in an argon matrix using 365 nm light (Supporting Information, Figure S1). However, the relative intensities of the UV−vis band at ca. 320 nm and IR peaks at 525, 923, and 1014 cm^{-1} are noticeably higher upon 365 nm irradiation.

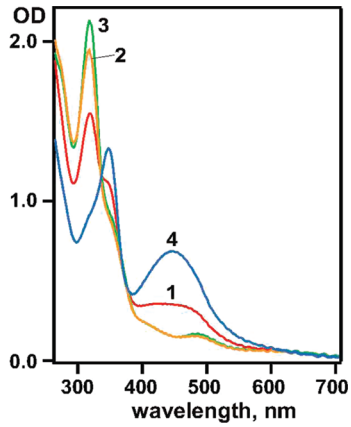

Figure 6. Changes in the UV−vis spectrum of intermediates, generated by the 15 min photolysis of **1** at 254 nm (1), upon 5 min (2), and the next 10 min (3) of irradiation at >405 nm and subsequent 313 nm photolysis during 15 min (4) in an argon matrix at 12 K.

Careful inspection of these spectra reveals that at least three intermediates (**2**−**4**) are formed upon irradiation of **1** at 254 nm in argon matrices. The primary intermediate **2** is responsible for the absorption maximum at approximately 320 nm and the IR peaks at 525, 923, and 1014 cm^{-1}. It is clear from Figure 5b that the yield of **2** decreases significantly with the time of irradiation. The second intermediate, **3**, has absorption maxima at 345 and approximately 450 nm and IR peaks at 581, 1053, and 1307 cm^{-1}. The yield of **3** grows with the time of irradiation. Most likely **3** is the product of a secondary photolysis. There are also some other IR peaks (at 726, 877, 883, 999 cm^{-1}), the intensities of which grow in concert with the decay of **1** (Figure 5b, negative peak at 948 cm^{-1}). These peaks provide an indication for a third product, **4**.

By irradiation of the samples, photolyzed previously at 254 (or 365) nm, at selected wavelengths we were able to induce and detect specific transformations of the intermediates **2**−**4** (Figures 6 and 7 or Supporting Information, Figure S2). Thus, spectrum 1 of Figure 6 was obtained from a sample irradiated at 254 nm for 15 min. According to the IR spectra, this photolysis led to 85% conversion of **1**. Further irradiation of this sample by visible light (>405 nm) resulted in the continued growth of the UV band at 318 nm and the decay of absorptions at 400−600 nm (Figure 6, spectra 2 and 3, and Figure 7a, spectrum 1). Subsequent photolysis of the same sample by UV light at 313 nm resulted in the growth of a new, broad band at 350−600 nm (Figure 6, trace 4, and Figure 7a, spectrum 2).

Figure 7b shows the corresponding changes in the IR spectrum. Photolysis at >405 nm (Figure 7b, trace 1) leads to the decay of IR peaks belonging to product **3** (581, 634, 1053, and 1307 cm^{-1}) and growth of the peaks of **2** and **4** as well as that of starting compound **1** (marked by asterisks). Subsequent 10 min of irradiation at >405 nm (Figure 7b, trace 2) led to the complete disappearance of **3** and to a small decrease of the peaks of **1** and **4**. Only product **2** is formed in the latter case. Its formation is accompanied by the growth of absorption at 318 nm and negligible decay in the visible region (Figure 6, spectrum 3).

In contrast, subsequent photolysis of the same sample, which contained **2**, **4**, and a small amount of **1**, at 313 nm resulted in the decay of all these species and exclusive formation of product **3** (Figure 7b, trace 3). The UV−vis spectrum of **3** (Figure 6, spectrum 4) has two maxima at 348 and 448 nm.

Hence, by means of selective UV or visible irradiations we were able to induce and detect the individual IR spectra of **3** (Figure 7b, negative peaks of trace 1 and positive peaks of trace 3) and **2** (Figure 7b, positive peaks of trace 2). Consequently, all IR peaks of **4** could also be identified. Moreover, the UV−vis spectrum of **3** was detected (Figure 6, spectrum 4). Unfortunately, it was impossible to discern the individual UV−vis spectra of **2** and **4**. It is only clear that both compounds absorb mainly in the UV region, with maxima around 320 nm (see also Supporting Information, Figure S1b).

To identify the structures of **2**−**4**, we performed quantum chemical calculations on a set of presumed intermediates, namely, different cyclic and acyclic isomers of starting compound **1**. Then we examined whether or not their calculated IR and UV spectra match with experiment. Thus we were able to select three intermediates, calculated IR spectra (Figure 7b, spectra 4−6) of which being in good agreement with the experimental spectra of species **2**−**4**. For example, Figure 7b shows that the IR spectrum of **3** is in good agreement with the calculated spectrum (trace 6) of

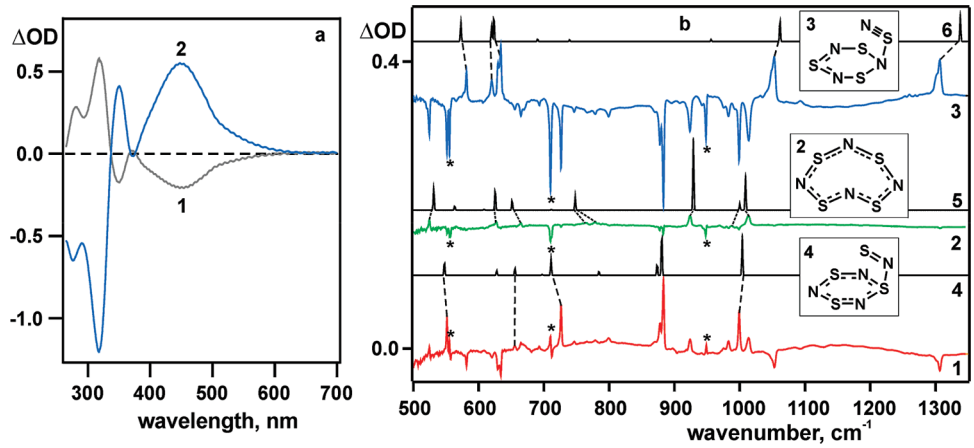

Figure 7. (a) Difference UV−vis spectra for the bleaching of intermediates (generated upon photolysis of **1** at 254 nm in an argon matrix at 12 K) on irradiation at >405 nm for 15 min (1) and 15 additional minutes at 313 nm (2). (b) Changes in the IR spectra of the intermediates formed after 15 min of photolysis of **1** at 254 nm upon further irradiation (>405 nm) for 5 min (1) and the next 10 min (2) and subsequent 313 nm photolysis during 15 min (3). The asterisks mark the positions of the experimental IR peaks of **1**. The traces 4−6 show the IR spectra of proposed intermediates predicted at the B3LYP/cc-pVTZ level.

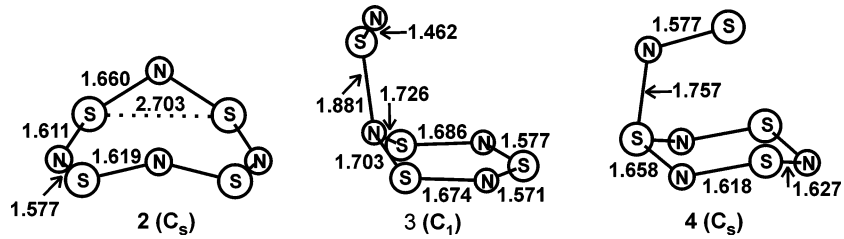

Figure 8. Bond lengths (in Å) of the intermediates **2**−**4** involved in the photoisomerization of **1**, optimized by the B3LYP/cc-pVTZ method. Symbols in parentheses indicate the point group of these structures.

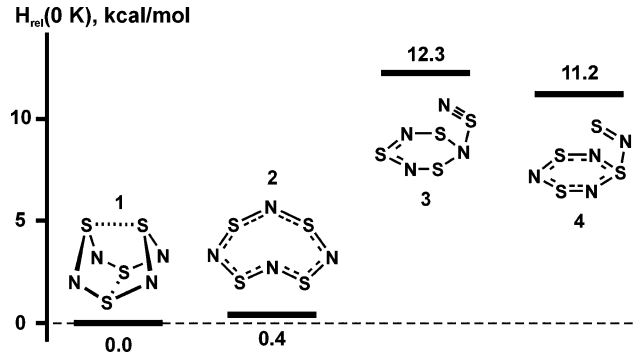

Figure 9. Relative 0 K enthalpies (in kcal/mol) of the species involved in the photoisomerization of **1**, calculated by the B3LYP/cc-pVTZ method.

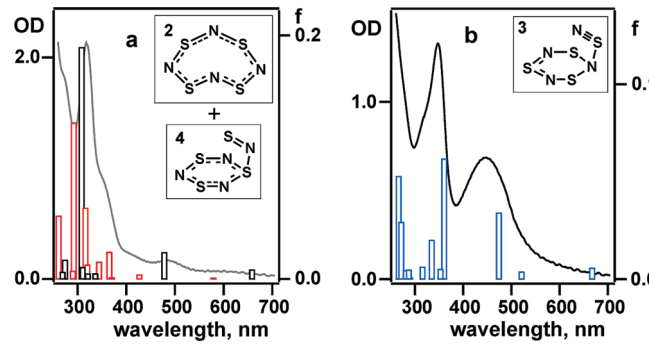

Figure 10. (a) UV−vis spectrum of the mixture of the intermediates **2** and **4** obtained after 15 min of irradiation at >405 nm in an argon matrix at 12 K. The vertical black and red open bars indicate the positions and oscillator strengths of electronic transitions of **2** and **4**, respectively, calculated by the TD-B3LYP/aug-cc-pVTZ method at the B3LYP/cc-pVTZ geometries. (b) UV−vis spectrum obtained upon 15 min of photolysis of intermediates **2** and **4** at 313 nm. The vertical blue open bars indicate the positions and oscillator strengths of the electronic transitions of **3** calculated by the TD-B3LYP/aug-cc-pVTZ method at the B3LYP/cc-pVTZ geometry.

the *cyclo*-S_3N_3—S≡N intermediate (Figure 8). According to the calculations the band at 1306 cm^{-1} belongs to the NS stretching mode. This value is in very good agreement with the experimental frequencies of NS vibrations measured for NSBr (1312 cm^{-1} in an argon matrix[24]) and NSCl (1327 cm^{-1} in an argon matrix,[24] 1322 cm^{-1} in CS_2,[25] and 1333, 1323.8, and 1316 cm^{-1} in the gas phase[26]), which support our assignment.

In turn, the IR spectrum of **2** coincides very well with the calculated spectrum (Figure 7, trace 5) of the lower symmetry (C_s) cyclic isomer of **1** (Figure 8) which has a boat structure resembling that of the well-known N-bonded adducts of **1** with some Lewis acids[1j] (e.g., $SbCl_5$,[1c,27] Supporting Information, Figure S3). A second, boat-shaped C_s conformation for cyclic S_4N_4 was recently found to be a local minimum on its potential energy surface,[3f] but the D_{2d} cage structure **1** was predicted to be favored by 2.4 and 0.3 kcal/mol at B3LYP/6-31+G(d) and MP4/6-31+G(d) levels, respectively. According to our calculations at the B3LYP/cc-pVTZ level ΔH_{rel} (0 K) amounts to a mere 0.4 kcal/mol (Figure 9).

Finally, all positive IR peaks of the trace 1 (Figure 7b), not identified as belonging to **2** and **1**, coincide well with

(24) Peake, S. C.; Downs, A. J. *J. Chem. Soc. Dalton* **1974**, 859–864.
(25) Nelson, J.; Heal, H. G. *Inorg. Nucl. Chem. Lett.* **1970**, *6*, 429–433.
(26) Muller, A.; Mohan, N.; Cyvin, S. J.; Weinstock, N.; Glemser, O. *J. Mol. Spectrosc.* **1976**, *59*, 161–170.
(27) Neubauer, D.; Weiss, J. *Z. Anorg. Allg. Chem.* **1960**, *303*, 28–38.

Scheme 1

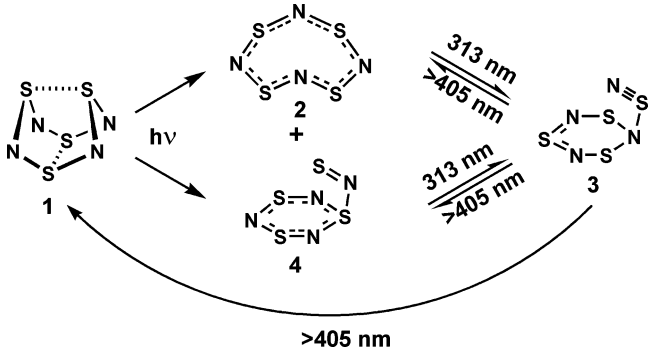

those in the spectrum calculated for the *cyclo*-S_3N_3—N═S structure, so we assign this structure to the intermediate **4** (Figure 8). Figure 9 shows that **4** is slightly more stable than the isomeric intermediate **3**.

Additional support of our assignment was obtained from a comparison of the experimental and calculated UV−vis spectra (Figure 10). Figure 10a shows the sum of the spectra of intermediates **2** and **4** (equal to trace 3 of Figure 6). Unfortunately, we found it impossible to reproduce the individual UV−vis spectra of **2** and **4** from our experimental data. Nevertheless, analyzing the difference spectrum of Figure S4 (Supporting Information), which corresponds to formation of the only product **2**, we can conclude that the absorption spectrum of **2** is slightly shifted to the red compared to that of **4**. The spectrum of intermediate **3**, displayed in Figure 10b (from trace 4 of Figure 6), coincides well with the calculated spectrum of the proposed *cyclo*-S_3N_3—S≡N structure. Moreover, the difference spectrum shown in Figure S4 of the Supporting Information, corresponding to the growth of **2**, is in very good agreement with the spectrum calculated for the proposed boat structure.

Therefore, the predominant primary products of **1** photolysis in argon matrices are its cyclic conformer **2** and its six-membered ring isomers **4** and **3**, respectively (Scheme 1). Thus, as proposed in the Introduction, the photochemical activation of **1**, similar to its reduction, promotes ring-opening and leads to the product of ring contraction (**4**). On continued UV irradiation the primary intermediates **2** and **4** undergo further transformation to the intermediate **3** (Scheme 1). The latter intermediate could be converted back to the primary products **2** and **4**, as well as to the starting **1**, upon irradiation by visible light (>405 nm).

Presently, little is known about the chemistry of RS≡N and RN═S derivatives except R = F.[28] The available scant data on structure, bonding, and, especially, the reactivity of such compounds are scattered and unsystematic.[29−32] However, it is clear that RS≡N and RN═S compounds are highly reactive and that this reactivity is responsible, at least in part, for the varied chemical properties of **1**.

A detailed investigation of the room-temperature photolysis of **1** using nanosecond laser flash photolysis, supplemented by appropriate quantum chemical calculations, is in progress, and the results of this study will be reported in due course.

Conclusions

In the present work we have studied the photochemical transformations of S_4N_4 (**1**) in argon matrices at 12 K using IR and UV−vis spectroscopy. Thereby, and with the help of quantum chemical calculations, we were able to conclude that under these experimental conditions the cage structure of **1** transforms into the isomeric structures **2**−**4**, one of which is the boat-shaped 8-membered cyclic isomer (**2**), whereas the other two are 6-membered S_3N_3 cycles carrying exocyclic −S≡N (**3**) or −N═S (**4**) groups, respectively. We found that these three isomeric compounds can be interconverted among each other, and with **1**, by irradiation at selected wavelengths (Scheme 1).

Most likely, **2** and **4** are the primary photolysis products. Formation of **4** from **1** could be imagined as proceeding by way of dissociation of a weak SN bond, followed by a recyclization. Formation of **2** requires dissociation of the weak transannular S−S bonds of **1**. Hence we propose two primary parallel photochemical processes, which imply the cleavage of an SN or SS bonds, respectively. According to our calculations on **1**, all transitions in the UV and visible regions (250−450 nm) consist of electron promotions to the doubly degenerate LUMO (12e), which is characterized as a combination of the σ^*(S−S) and π^*(S−N) antibonding orbitals (Figure 4). This finding correlates with the discovered photochemistry of **1**.

Since the electronic excitation or reduction of **1**, as well as its reactions with nucleophiles, all result in the population of the LUMO, the formation of a 6-membered S_3N_3 ring upon photolysis is in accordance with the well-known ring contraction that occurs under the influence of nucleophilic or reducing agents.

Acknowledgment. The authors are grateful to the Russian Foundation for Basic Research (Project 07-03-00467), the Siberian Branch of the Russian Academy of Sciences (interdisciplinary Project No. 25), and the Swiss National Science Foundation (Project No. 200020-113268) which

(28) Glemser, O.; Mews, R. *Angew. Chem., Int. Ed.* **1980**, *19*, 883–899.
(29) (a) Hartmann, G.; Mews, R.; Sheldrick, G. M.; Anderskewitz, R.; Niemeyer, M.; Emeleus, H. J.; Oberhammer, J. *J. Fluorine Chem.* **1986**, *34*, 46–58. (b) Haas, A.; Mischo, T. *Can. J. Chem.* **1989**, *67*, 1902–1908. (c) Maggiulli, R.; Lork, E.; Behrens, U.; Burger, K.; Mews, R. *J. Fluorine Chem.* **2000**, *102*, 337–343.
(30) (a) Zibarev, A. V.; Lork, E.; Mews, R. *Chem. Commun.* **1998**, 991–992. (b) Borrmann, T.; Zibarev, A. V.; Lork, E.; Knitter, G.; Chen, S.-J.; Watson, P. G.; Cutin, E.; Shakirov, M. M.; Stohrer, W.-D.; Mews, R. *Inorg. Chem.* **2000**, *39*, 3990–4005. (c) Borrmann, T.; Lork, E.; Mews, R.; Stohrer, W.-D.; Watson, P. G.; Zibarev, A. V. *Chem. Eur. J.* **2001**, *7*, 3504–3510. (d) Borrmann, T.; Lork, E.; Shakirov, M. M.; Zibarev, A. V. *Eur. J. Inorg. Chem.* **2004**, 2452–2458.
(31) (a) Yoshimura, T. *Rev. Heteroatom Chem.* **2000**, *22*, 101–120. (b) Fujii, T.; Itoh, A.; Hamata, K.; Yoshimura, T. *Tetrahedron Lett.* **2001**, *42*, 5041–5043.
(32) (a) Pedersen, C. L.; Lohse, C.; Poliakoff, M. *Acta Chem. Scand. B* **1978**, *32*, 625–631. (b) Joucla, M. F.; Rees, C. W. *Chem. Commun.* **1984**, 374–375. (c) Okazaki, R.; Takahashi, M.; Inamoto, N.; Sugawara, T.; Iwamura, H. *Chem. Lett.* **1989**, *12*, 2083–2086. (d) Takahashi, M.; Okazaki, R.; Inamoto, N. *Chem. Lett.* **1989**, *12*, 2087–2090. (e) Takahashi, M.; Okazaki, R.; Inamoto, N.; Sugawara, T.; Iwamura, H. *J. Am. Chem. Soc.* **1992**, *114*, 1830–1837.

made it possible for E.A.P. to visit Fribourg University under the SCOPES program and carry out the experiments and calculations described in this paper.

Supporting Information Available: Cartesian coordinates of all stationary points located in this study, positions and oscillator strengths of transitions for compounds **1**−**4** calculated by the B3LYP/aug-cc-pVTZ//B3LYP/cc-pVTZ method in argon, UV−vis and IR spectra recorded upon irradiation of **1** in an argon matrix by a 365 nm light (Figures S1 and S2), experimental structure of N-bonded adduct of **1** with $SbCl_5$[27] (Figure S3), and difference UV−vis spectrum corresponding to formation of the only product **2** (Figure S4). This material is available free of charge via the Internet at http://pubs.acs.org.

IC802145X